



Wave collapse in a class of nonlocal nonlinear Schrödinger equations

Mark Ablowitz^a, İlkay Bakırtaş^b, Boaz Ilan^{a,*}

^a *Department of Applied Mathematics, University of Colorado, Campus Box 526, Boulder, CO 80309-0526, USA*

^b *Department of Mathematics, Istanbul Technical University, Maslak 34469, Istanbul, Turkey*

Received 10 October 2004; received in revised form 30 March 2005; accepted 3 June 2005

Available online 22 June 2005

Communicated by A.C. Newell

Abstract

Wave collapse is investigated in nonlocal nonlinear Schrödinger (NLS) systems, where a nonlocal potential is coupled to an underlying mean term. Such systems, here referred to as NLS-Mean (NLSM) systems, are also known as Benney–Roskes or Davey–Stewartson type and they arise in studies of shallow water waves and nonlinear optics. The role of the ground-state in global-existence theory is elucidated. The ground-state is computed using a fixed-point method. The critical-powers for collapse predicted by the Virial Theorem, global-existence theory, and by direct numerical simulations of the NLSM are found to be in good agreement with each other for a wide range of parameters. The ground-state profile in the water-wave case is found to be generically narrower along the direction of propagation, whereas in the optics case it is generically wider along the axis of linear polarization. In addition, numerical simulations show that NLSM collapse occurs with a quasi self-similar profile that is a modulation of the corresponding astigmatic ground-state, which is in the same spirit as in NLS collapse. It is also found that NLSM collapse can be arrested by small nonlinear saturation.

© 2005 Elsevier B.V. All rights reserved.

Keywords: Blowup; Singularity formation; Modulated nonlinear waves

1. Introduction

Nonlinear waves problems are of wide physical and mathematical interest and arise in a variety of scientific fields such as nonlinear optics, fluid dynamics, plasma physics, etc. (cf. [7,36]). The solutions of the governing nonlinear

* Corresponding author. Tel.: +1 303 492 4543; +1 303 492 4066.

E-mail address: boaz@colorado.edu (B. Ilan).

waves equations often exhibit important phenomena, such as stable localized waves (e.g., solitons), self-similar structures, chaotic dynamics and wave singularities such as shock waves (derivative discontinuities) and/or wave collapse (i.e., blowup) where the solution tends to infinity in finite time or finite propagation distance. A prototypical equation that arises in *cubic media*, such as Kerr media in optics, is the (2+1)D focusing cubic nonlinear Schrödinger equation (NLS),

$$iu_z(x, y, z) + \frac{1}{2}\Delta u + |u|^2u = 0, \quad u(x, y, 0) = u_0(x, y), \quad (1)$$

where u is the slowly-varying envelope of the wave, z is the direction of propagation,¹ (x, y) are the transverse directions, $\Delta u \equiv u_{xx} + u_{yy}$, and u_0 is the initial conditions. Remarkably, in 1965 Kelley [23] carried out direct numerical calculations of (1) that indicated the possibility of wave collapse. In 1970, Vlasov et al. [34] proved that solutions of Eq. (1) satisfy the following “Virial Theorem” (also called Variance Identity)

$$\frac{d^2}{dz^2} \int (x^2 + y^2)|u|^2 = 4H, \quad H = \frac{1}{2} \int (|\nabla u_0|^2 - |u_0|^4), \quad (2)$$

where $\nabla \equiv (\partial_x, \partial_y)$, the integrations are carried over the (x, y) plane, and H , which is a constant of motion, is the Hamiltonian of Eq. (1). Using the Virial Theorem, Vlasov et al. concluded that the solution of the NLS can become singular in finite distance (or time), because a positive-definite quantity could become negative for initial conditions satisfying $H < 0$. On the other hand, Weinstein [35] showed that when the power (which is also conserved) is sufficiently small, i.e., $N = \int |u_0|^2 = \text{constant} < N_c \approx 1.8623\pi$, the solution exists globally, i.e., for all $z > 0$. Therefore, a *sufficient condition* for collapse is $H < 0$ while a *necessary condition* for collapse is $N > N_c$. Weinstein also found that the *ground-state* of the NLS plays an important role in the collapse theory. This ground-state is a “stationary” solution of the form $u = R(r)e^{iz}$, such that R is radially-symmetric, positive, and monotonically decaying. Papanicolaou et al. [27] studied the singularity structure near the collapse point and showed asymptotically and numerically that collapse occurs with a (quasi) self-similar profile. The readers are referred to [30] for a comprehensive review of related studies. Recent research by Merle and Raphael [26] further elaborated on the collapse behavior of NLS Eq. (1) and related equations, allowing for detailed understanding of the self-similar asymptotic profile. Furthermore, Gaeta and coworkers [24] recently carried out detailed optical experiments in cubic media that reveal the nature of the singularity formation and showed experimentally that collapse occurs with a self-similar profile.

On the other hand, there are considerably fewer studies of wave collapse that arises in nonlinear media, whose governing system of equations have *quadratic nonlinearities*, such as water waves and $\chi^{(2)}$ nonlinear-optical media. Here we discuss a class of such systems, denoted as NLS-Mean (NLSM) systems, which are sometimes referred to as Benney and Roskes [8] or Davey and Stewartson [13] type. The physical derivation of NLSM systems in water waves and nonlinear optics is reviewed in Section 2. Broadly speaking, the derivation of NLSM systems is based on an expansion of the slowly-varying (i.e., quasi-monochromatic) wave amplitude in the first and second harmonics of the fundamental frequency, as well as a mean term that corresponds to the zeroth harmonic. This leads to a system of equations that describes the nonlocal-nonlinear coupling between a dynamic field that is associated with the first harmonic (with a “cascaded” effect from the second harmonic), and a static field that is associated with the mean term (i.e., the zeroth harmonic). For the physical models considered in this study, the general NLSM system can be written in the following non-dimensional form,

$$iu_z + \frac{1}{2}(\sigma_1 u_{xx} + u_{yy}) + \sigma_2 u |u|^2 - \rho u \phi_x = 0, \quad \phi_{xx} + \nu \phi_{yy} = (|u|^2)_x, \quad (3)$$

where $u(x, y, t)$ corresponds to the field associated with the first-harmonic, $\phi(x, y, t)$ corresponds to the mean field, σ_1 and σ_2 are ± 1 , and ν and ρ are real constants that depend on the physical parameters. It is well-known

¹ In this study z plays the role of the evolution variable (i.e., like time).

that System (3) can admit collapse of localized waves when $\sigma_1 = \sigma_2 = 1$ and $\nu > 0$. In that case, the governing equations are

$$iu_z + \frac{1}{2}\Delta u + |u|^2 u - \rho u \phi_x = 0, \quad (4a)$$

$$\phi_{xx} + \nu \phi_{yy} = (|u|^2)_x, \quad (4b)$$

where $\nu > 0$ and ρ is real, and the initial conditions are $u(x, y, 0) = u_0(x, y)$, $\phi(x, y, 0) = \phi_0(x, y)$, such that Eq. (4b) is satisfied at $z = 0$, i.e., $\phi_{0,xx} + \nu \phi_{0,yy} = (|u_0|^2)_x$. The goal of this study is to further investigate the collapse dynamics in the NLSM System (4).

We note that System (4) reduces to the classical NLS Eq. (1) when $\rho = 0$, because in that case the mean field ϕ does not couple to the harmonic field u in Eq. (4a). In addition, when $\nu = 0$ Eq. (4b) gives that $\phi_x = |u|^2$ and, therefore, Eq. (4a) reduces to a classical NLS Eq. (1) with the cubic term $(1 - \rho)|u|^2 u$. As we shall see, in optics $\rho > 0$, whereas in water waves $\rho < 0$. In either case, i.e., when $\rho \neq 0$, the NLSM System (4) is a nonlocal system of equations. Indeed, since $\nu > 0$, Eq. (4b) can be solved as

$$\phi(x, y, z) = \int_{-\infty}^{\infty} G(x - x', y - y') \frac{\partial}{\partial x'} |u(x', y', z)|^2 dx' dy',$$

where $G(x, y)$ is the usual Green's function. For Eq. (4b) $G(x, y) = (4\pi)^{-1} \log(x^2 + y^2/\nu)$, which corresponds to a strongly-nonlocal function ϕ . While one might have expected the strong-nonlocality in the NLSM to arrest the collapse process, generally speaking, that is not the case for System (4). Moreover, there is a striking mathematical similarity between collapse dynamics in the NLS and NLSM cases.

The paper is organized as follows:

- (1) In Section 2 NLSM systems in water waves and in nonlinear optics are discussed.
- (2) In Section 3 the theory of collapse and global existence in NLS and NLSM equations is reviewed. In addition, the Hamiltonian is used to explain why collapse in the case of water waves ($\rho < 0$) is relatively easier to attain, and also occurs more quickly, than in the case of nonlinear optics ($\rho > 0$).
- (3) Using global existence theory and numerical calculations of the ground-state, in Section 4 the necessary condition for collapse is explored in terms of the parameters ν and ρ in the NLSM System (4). Using the Virial Theorem and the Hamiltonian, a sufficient condition for collapse is found for Gaussian input beams, explicitly in terms of ν , ρ , and the input power. These theoretical results are found to be consistent with numerical simulations of the NLSM System (4) and are also consistent with the numerical results of Crasovan et al. [12] for nonlinear optics ($\rho > 0$). In addition, the effect of input astigmatism in the initial conditions on the critical power for collapse is studied (Section 4.1). Furthermore, in Section 4.2 it is shown that the NLSM can admit collapse even without the cubic term [i.e., without $|u|^2 u$ in Eq. (4a)].
- (4) In Section 5 the astigmatism of the NLSM ground-state is explored in the (ν, ρ) parameter space. It is found that the ground-state is relatively more astigmatic for nonlinear optics ($\rho > 0$) than for water waves ($\rho < 0$). In addition, the dependence of the astigmatism of the ground-state on ν is found to be weaker than its dependence on ρ .
- (5) In Section 6 simulations of the NLSM System (4) show that the collapsing solution is well described by a quasi self-similar profile that is given in terms of a modulation of the corresponding ground state, a result that is in the same spirit as for the NLS equation and also strengthens the results of Papanicolaou et al. [28]. However, in [28] the ground-state itself was not computed and, in turn, it was not shown numerically that the asymptotic profile approaches the corresponding ground-state. In this study numerical simulations directly show that the collapsing wave approaches a quasi self-similar modulation of the corresponding ground-state. To calculate the ground-state a fixed-point algorithm is used, which has been previously applied in dispersion-managed NLS theory (see Appendix C).

- (6) In Section 7 numerical simulations are used to show that NLSM collapse can be arrested by a small saturation of the cubic nonlinearity, a phenomenon that can be explained using the results of Fibich and Papanicolaou [19] for the the perturbed NLS.

2. NLSM systems in water waves and nonlinear optics

Below we review some of the main results from the derivations of NLSM systems, with an emphasis on collapse.

2.1. Water waves

In the context of free-surface gravity-capillary water waves, NLSM equations result from a weakly-nonlinear quasi-monochromatic expansion of the velocity potential as

$$\phi(x, y, t) \sim \varepsilon[\tilde{A}e^{i(kx- \omega t)} + \text{c.c.} + \tilde{\Phi}] + \varepsilon^2[\tilde{A}_2e^{2i(kx- \omega t)} + \text{c.c.}] + \dots, \tag{5}$$

where x is the direction of propagation, y the transverse direction, t the time, $\varepsilon \ll 1$ a measure of the (weak) nonlinearity, \tilde{A} , \tilde{A}_2 , and $\tilde{\Phi}$ are slowly varying functions of (x, y, t) , which correspond to the coefficients of the first, second, and zeroth harmonics, respectively, “c.c.” denotes complex conjugate of the term to its left, and the frequency ω satisfies the dispersion relation $\omega^2(\kappa) = (g\kappa + T\kappa^3) \tanh(\kappa h)$, where g is the gravity acceleration, T is the surface tension coefficient, and $\kappa = \sqrt{k^2 + l^2}$, where (k, l) are the wave-numbers in the (x, y) directions, respectively. Substituting the wave expansion (5) into the water-wave equations (i.e., Euler’s equation with a free surface) and assuming slow modulations of the field in the x and y directions results in a nonlinearly-coupled system for \tilde{A} and $\tilde{\Phi}$. After non-dimensionalization, i.e., $(A, \Phi) = (\tilde{A}, \tilde{\Phi})k^2/\sqrt{gh}$, one finds the general NLSM system [6]

$$iA_\tau + \lambda A_{\xi\xi} + \mu A_{\eta\eta} = \chi|A|^2A + \chi_1A\Phi_\xi, \tag{6a}$$

$$\alpha\Phi_{\xi\xi} + \Phi_{\eta\eta} = -\beta(|A|^2)_\xi, \tag{6b}$$

where $\xi = \varepsilon k(x - c_g t)$, $\eta = \varepsilon ly$ and $\tau = \varepsilon^2 \sqrt{gk} t$ are dimensionless coordinates, and $c_g = \partial\omega/\partial k$ is group velocity. The coefficients $\lambda, \mu \geq 0$, $\chi, \chi_1 \geq 0$, α and $\beta \geq 0$ are suitable functions of h, T, k, c_g , and the second-order dispersion coefficients $\partial^2\omega/\partial k^2$ and $\partial^2\omega/\partial l^2$. We note that in the derivation of System (6) \tilde{A}_2 is expressed in terms of \tilde{A} , which accounts for the fact that A_2 does not appear explicitly in the resulting system.²

NLSM equations were originally obtained by Benney and Roskes [8] in their study of the instability of wave packets in water of finite depth h , without surface tension. In 1974, Davey and Stewartson [13] studied the evolution of a 3D wave packet in water of finite depth and obtained a different, although equivalent, form of these equations. In 1975 Ablowitz and Haberman [4] studied the integrability of systems such as (6). These integrable systems correspond to the Benney–Roskes equations in the shallow water limit. In 1977, Djordevic and Reddekopp [14] extended the results of Benney and Roskes to include surface tension. Subsequently, Ablowitz and Segur [6] investigated System (6) or, equivalently, System (3). They showed that the shallow water limit, i.e., $h \rightarrow 0$, corresponds to $\sigma_1 \rightarrow -\nu = \pm 1$, and $\rho \rightarrow 2$ in System (3). The resulting equations agreed with those obtained by Ablowitz and Haberman [4]. Hence, the shallow-water limit of System (6) is integrable and can be obtained from an associated compatible linear scattering system. In [21] these reduced equations were linearized by the inverse scattering transform (see also [3]).

Subsequently, Ablowitz and Segur [6] studied the NLSM System (6) in the non-integrable case. In this parameter regime, System (6) can be transformed by a rescaling of variables to System (3) with $\sigma_1 = \sigma_2 = 1$ and $\nu > 0$, i.e.,

² A similar observation holds in the optics case mentioned below.

the so called focusing elliptic–elliptic case, which, physically speaking, requires sufficiently large surface tension. They found that System (6) preserves the Hamiltonian

$$H = \int \left[\lambda \left| \frac{\partial A}{\partial \xi} \right|^2 + \mu \left| \frac{\partial A}{\partial \eta} \right|^2 \right] - \frac{1}{2} \int \left[(-\chi) |A|^4 + \frac{\alpha \chi_1}{\beta} (\Phi_\xi)^2 + \frac{\chi_1}{\beta} (\Phi_\eta)^2 \right], \quad (7)$$

where the first and second integrals correspond to the second-derivative and the nonlinear terms in Eq. (6a), respectively, and the integrations are carried over the (ξ, η) plane. When, in addition to the physical requirements $\mu \geq 0$, $\beta \geq 0$, and $\chi_1 \geq 0$, one has that $\lambda > 0$, $-\chi > 0$, and $\alpha > 0$, the first and second integral terms in (7) are positive and negative-definite, respectively. This corresponds to the self-focusing regime. Clearly, in that case $H < 0$ is possible for sufficiently large initial conditions.³ Furthermore they proved that the following Virial Theorem holds

$$\frac{\partial^2}{\partial \tau^2} \int \left(\frac{\xi^2}{\lambda} + \frac{\eta^2}{\mu} \right) |A|^2 = 8H.$$

As can be seen, if $H < 0$, the moment of inertia vanishes at a finite time. In that case, as for the NLS case mentioned above, this indicates finite-distance singularity formation. We note that in the same study collapse solutions with the self-similar profile were also investigated, i.e., with $|A| \sim L^{-1} f(\frac{x}{L}, \frac{y}{L})$, where $L = L(t)$ approaches zero during the collapse.

2.2. Nonlinear optics

The electric polarization field of intense laser beams propagating in optical media can be expanded in powers of the electric field as

$$P = \chi^{(1)} \times E + \chi^{(2)} \times E \times E + \chi^{(3)} \times E \times E \times E + \dots, \quad (8)$$

where $E = (E_1, E_2, E_3)$ the electric field vector and $\chi^{(j)}$ are the susceptibility tensor coefficients of the medium. In isotropic Kerr media, where the nonlinear response of the material depends cubically [i.e., through $\chi^{(3)}$ and when $\chi^{(2)} \equiv 0$] and instantaneously on the applied field, the dynamics of a quasi-monochromatic optical pulse is governed by the NLS Eq. (1) (cf. [9,23,31]). It turns out that NLSM type equations also arise in nonlinear optics when studying media with a non-zero $\chi^{(2)}$ [even when $\chi^{(3)} \equiv 0$], i.e., materials that have a *quadratic* nonlinear response. Such materials are anisotropic, e.g., crystals whose optical refraction has a preferred direction.

Ablowitz et al. [1,2] found, from first principles, that NLSM type equations describe the evolution of the electromagnetic field in such quadratically [i.e., $\chi^{(2)}$] polarized media. Both scalar and vector (3+1)D NLS systems were obtained. Briefly, in this derivation one assumes a quasi-monochromatic expansion of the x component of the electromagnetic field (which is primarily linearly-polarized), with the fundamental harmonic, second-harmonic, and a mean term as

$$E_1 \sim \varepsilon [A e^{i(kx - \omega t)} + \text{c.c.}] + \varepsilon^2 [A_2 e^{2i(kx - \omega t)} + \text{c.c.} + \phi_x] + \dots, \quad (9)$$

where A , A_2 , and ϕ are slowly varying functions of (x, y, t) , which correspond to the first, second, and zeroth harmonics, respectively. Using a polarization field of the form (8) in Maxwell's equations leads to the system of equations

$$[2ik\partial_Z + (1 - \alpha_{x,1})\partial_{XX} + \partial_{YY} - kk''\partial_{TT} + M_{x,1}|A|^2 + M_{x,0}\phi_x]A = 0, \quad (10a)$$

$$[(1 - \alpha_{x,0})\partial_{XX} + \partial_{YY} + s_x\partial_{TT}]\phi_x - \alpha_{y,0}\partial_{XY}\phi_y = (N_{x,1}\partial_{TT} - N_{x,2}\partial_{XX})|A|^2, \quad (10b)$$

³ Note that from Eq. (6b) Φ scales as $|A|^2$, so all the terms in the second integral of (7) scale like $|A|^4$.

where $\alpha_{x,0}$, $\alpha_{x,1}$, $\alpha_{y,0}$, and s_x depend on the linear polarization term $\chi^{(1)}$; $M_{x,0}$, $N_{x,1}$, and $N_{x,2}$ depend on the nonlinear polarization terms $\chi^{(2)}$ and $\chi^{(3)}$; and $M_{x,1}$ depends on products of $\chi^{(2)}$ and $\chi^{(3)}$. Physically speaking, the dependence of $M_{x,1}$ on $\chi^{(2)}$ and $\chi^{(3)}$ corresponds to the fact that the second-harmonic (i.e., \tilde{A}_2) is coupled to the first harmonic (i.e., \tilde{A}_1), a process that is sometimes referred to as “optical rectification” or “cascaded” optical effect. However, as in the water-wave case, here too \tilde{A}_2 is expressed in terms of \tilde{A} , which is why A_2 does not appear explicitly in the resulting system (10). In addition, similar to the water-wave case, the term with $M_{x,0}$ in System (10a) couples the mean field to the first-harmonic field. Interestingly, when the time dependence in these equations is neglected ($\partial_T \equiv 0$) and for media with a special symmetry class such that $\alpha_{y,0} = 0$, it can be seen that, after proper rescaling, the governing system of equation is given by System (4). In [32] these equations were further elucidated and the coefficients described in terms of the electro-optic effect.

From the point of view of perturbation analysis, it is interesting to remark that in the expansion of the field in the case of water-waves [i.e., Eq. (5)], the mean term $\tilde{\Phi}$ appears as an $O(\varepsilon)$ term, whereas in the in the case of optics [i.e., Eq. (9)], the mean term ϕ_x appears as an $O(\varepsilon^2)$ term. However, the physically measurable quantity in water waves is $\tilde{\Phi}_x$, which scales like $O(\varepsilon^2)$, because $\tilde{\Phi}$ is slowly-varying. Therefore, the expansions in the water-wave and optics cases are, in fact, analogous from the viewpoint of perturbation analysis.

Wave collapse in such NLSM systems was recently investigated numerically by Crasovan et al. [12]. They solved the following normalized system of equations,

$$iU_z + \frac{1}{2}\Delta U + |U|^2U - \rho UV = 0, \tag{11a}$$

$$V_{xx} + \nu V_{yy} = (|U|^2)_{xx}, \tag{11b}$$

where U is the normalized amplitude of the envelope of the electric field, V the normalized static field, ρ a coupling constant that comes from the combined optical rectification and electro-optic effects, and ν corresponds to the anisotropy coefficient of the medium. They solved System (11) numerically with Gaussian initial conditions for U . The regions of collapse were investigated for various values of the parameters ρ and ν . We note that System (11) is a simple mathematical modification of the NLSM System (4). Indeed, starting with the NLSM System (4), taking the derivative of Eq. (4b) with respect to x , and defining the new variable (potential) $V = \phi_x$, one finds that the resulting system is identical to (11).

3. Global existence, collapse, and the ground-state

We begin by briefly outlining some of the known results for the NLS and NLSM equations. Two conserved quantities for the NLS Eq. (1) and NLSM System (4) are the power, i.e.,

$$N(u) = \int |u|^2 = N(u_0), \tag{12}$$

where the integrations (here and below) are carried over the (x, y) plane, and the Hamiltonian, i.e.,

$$H_{\text{NLS}}(u) = \frac{1}{2} \int |\nabla u|^2 - \frac{1}{2} \int |u|^4 = H_{\text{NLS}}(u_0),$$

$$H_{\text{NLSM}}(u, \phi) = \frac{1}{2} \int |\nabla u|^2 - \frac{1}{2} \int |u|^4 + \frac{\rho}{2} \int (\phi_x^2 + \nu \phi_y^2) = H_{\text{NLSM}}(u_0, \phi_0), \tag{13}$$

where H_{NLS} and H_{NLSM} correspond to Eq. (1) and System (4), respectively, and ϕ in (13) is obtained from Eq. (4b). In addition, the Virial Theorem holds (cf. [6]),

$$\frac{\partial^2}{\partial z^2} \int (x^2 + y^2)|u|^2 = 4H, \tag{14}$$

where H is the corresponding Hamiltonian, i.e., either H_{NLS} or H_{NLSM} . We are interested in the localized-decaying case, when u and ϕ vanish sufficiently rapidly at infinity to be in the Sobolev space H_1 , i.e., $\int |u|^2 + \int |\nabla u|^2 < \infty$ and similarly for ϕ . We note that within the context of the water-wave problem (i.e., $\rho < 0$), existence and well-posedness of solutions of System (4) were studied in [22]. Singularity formation corresponds to finite-time (or finite-distance) blowup in H_1 . Since the L_2 norm is conserved (12), blowup in H_1 amounts to $\lim_{z \rightarrow Z_c} \int |\nabla u|^2 = \infty$, where Z_c is the collapse distance. In fact, it is well-known in NLS and NLSM theories that when a singularity occurs, the peak amplitude of the wave blows-up as well, i.e., $\lim_{z \rightarrow Z_c} \max_{(x,y)} |u(x, y, z)| = \infty$.

When $H < 0$ it follows from the Virial Theorem (14) that the solution becomes singular in finite time. This gives a *sufficient condition* for collapse. On the other hand, a *necessary condition* for collapse can be obtained using the associated ground-state, as reviewed below. We note that the Hamiltonian (13) is comprised of three integrals, the first of which is positive definite, the second negative definite, and, when $\nu \geq 0$, the third integral is definite with a sign that is determined by ρ . Generally speaking, NLS (and NLSM) theory shows that the positive-definite terms correspond to defocusing mechanisms, while the negative-definite terms correspond to focusing mechanisms. Thus, it follows that when $\rho > 0$, i.e., in the optics case, the coupling to the mean field corresponds to a self-defocusing mechanism, while when $\rho < 0$, i.e., the water-wave case, it corresponds to a self-focusing effect in addition to the cubic term in the NLS Eq. (1). In other words, loosely speaking, one can expect that self-focusing in the water-wave case is “easier” to attain than in the optics case (see Sections 4 and 6 for details).

A stationary solution of the NLSM System (4) is a solution of the form $u(x, y, z) = F(x, y)e^{i\lambda z}$ and $\phi(x, y, z) = G(x, y)$, where F and G are real functions and λ is a positive real number. Substituting this ansatz into System (4) gives

$$-\lambda F + \frac{1}{2}\Delta F + F^3 - \rho FG_x = 0, \tag{15a}$$

$$G_{xx} + \nu G_{yy} = (F^2)_x. \tag{15b}$$

Similarly, the NLS stationary solutions, which are obtained by substituting $u = R(x, y)e^{i\lambda z}$ into the NLS Eq. (1), satisfy

$$-\lambda R + \frac{1}{2}\Delta R + R^3 = 0. \tag{16}$$

The *ground-state* of the NLS⁴ can be defined as a solution in H_1 of Eq. (16) for a given λ having minimal power of all the nontrivial solutions. The existence and uniqueness of the ground state have been proven, as also the fact that it is radially-symmetric, positive, and monotonically decaying (see [30]). Since $R(r; \lambda) = \sqrt{\lambda}R(\sqrt{\lambda}r; 1)$, it suffices to consider the case $\lambda = 1$, for which the solution is henceforth denoted by R . Furthermore, Weinstein [35] proved that the NLS ground-state is a minimizer of a Gagliardo-Nirenberg inequality that is associated with the NLS Hamiltonian. To be precise, the functional

$$J(u) = \frac{\|u\|_2^2 \|\nabla u\|_2^2}{\|u\|_4^4}, \quad \|u\|_p^p \equiv \int |u|^p,$$

attains its minimum for $u \in H_1$ when $u(x, y) = R(r)$, where R is the ground-state of Eq. (16) and $J(R) = 2/N_c$, where $N_c \equiv \int R^2$. Moreover, Weinstein proved that when $N < N_c$, the NLS solution exists globally (i.e., for all $z > 0$) in H_1 . In addition, it is not difficult to show (cf. Appendix A) that any stationary solution, in particular the ground-state, admits a zero Hamiltonian, i.e., $H_{\text{NLS}}(R) = 0$. These results can be used to explain why the ground-state may be considered to be on the borderline between existence and collapse. Indeed, consider the initial conditions $u_0 = (1 + \varepsilon)R(r)$ with $\varepsilon = \text{constant}$. When $\varepsilon < 0$ then $N < N_c$ and, therefore, the solution exists globally. On the other hand, when $\varepsilon > 0$ then $H < 0$ and, therefore, finite-distance collapse is guaranteed by the Virial Theorem

⁴ R , the NLS ground-state, is sometimes referred to as the Townes profile.

(cf. [35]). We note that $N \geq N_c$ is only a necessary condition for collapse, i.e., there are solutions with $N > N_c$ that exist globally.

Similarly to the NLS case, the ground-state of System (15) can be defined as the nontrivial solution (F, G) in H_1 , such that F has minimal power. Cipolatti [10] proved the existence of the ground-state. In the same spirit as for the NLS, Papanicolaou et al. [28] defined the ground-state as the minimizer the associated functional⁵

$$J(u) = \frac{\|u\|_2^2 \|\nabla u\|_2^2}{\int[|u|^4 + \mathcal{B}(u)u^{*2}]}, \quad \mathcal{B}(u) \equiv \mathcal{F}^{-1} \left[\frac{\rho k_x^2}{k_x^2 + \nu k_y^2} \mathcal{F}[|u|^2] \right],$$

where \mathcal{F} and \mathcal{F}^{-1} denote the Fourier Transform operator and its inverse, respectively (see Appendix B). They extended global existence theory to the NLSM and proved the following.

Theorem 3.1. Consider System (4) with initial conditions $u_0 \in H_1$. Let F be the nontrivial minimizer of $J(u)$ above, and let N_c be defined as

$$N_c(\nu, \rho) \equiv \int F^2(x, y; \nu, \rho). \tag{17}$$

Then F is a positive function and, therefore, $N_c > 0$. In addition, if $\int |u_0|^2 < N_c$ the solution of System (4) exists in H_1 for all $z > 0$.

In other words, solutions of the NLSM System (4) exist globally when their power is smaller than the power of the corresponding ground-state.

On the other hand, since the ground-state is a stationary solution, in analogy to $H_{\text{NLS}}(R) = 0$, one has also (see Appendix A)

Proposition 3.2. Let (F, G) be a solution of System (15). Then

$$H_{\text{NLSM}}(F, G) \equiv \frac{1}{2} \int (\nabla F)^2 - \frac{1}{2} \int F^4 + \frac{\rho}{2} \int (\nabla_\nu G)^2 = 0, \tag{18}$$

where $(\nabla_\nu G)^2 \equiv G_x^2 + \nu G_y^2$.

Therefore, it follows from Theorem 3.1, the Virial Theorem (14), and Proposition 3.2 that, as in the NLS case, the NLSM ground-state is neutrally-stable and may be considered to be on the borderline between global existence and collapse.

4. Collapse and global-existence regions

In this section System (4) is considered with the Gaussian initial conditions

$$u_0^G(x, y) = \sqrt{\frac{2N}{\pi}} e^{-(x^2+y^2)}, \tag{19}$$

where $N = N(G)$ is the input power of u_0^G . The collapse and global-existence regions in the NLSM System (4) are explored in the (N, ν, ρ) parameter space using the results obtained from the Virial Theorem (14), the global-existence Theorem (3.1), and direct (2+1)D numerical simulations of the NLSM System (4).

⁵ Note that from Eq. (4b) $\phi_x = \rho^{-1} \mathcal{B}(u)$.

The critical power $N_c(\nu, \rho)$ is calculated from the ground-state [see Eq. (17)], which is found by using a numerical method that is explained in Appendix C. For the NLSM simulations a standard fourth order accurate Runge-Kutta integration is used, with a fourth order accurate spatial finite-difference stencil. The computational domain is a truncation of the (x, y) plane with Dirichlet boundary-conditions at $|x| = L$ and $|y| = L$, where L is taken sufficiently large, so to assure that the results are independent of reflections from the outer boundaries.

Substituting the initial-conditions (19) into the NLSM Hamiltonian (13) gives (see Appendix B)

$$H(u_0^G, \phi_0^G) = N - \left(1 - \frac{\rho}{1 + \sqrt{\nu}}\right) \frac{N^2}{2\pi}. \tag{20}$$

It follows from (20) and the Virial Theorem (14) that for the Gaussian initial conditions (19) there is a *threshold power* for which $H = 0$, given by

$$N_c^H(\nu, \rho) \equiv \frac{2\pi}{1 - \rho/(1 + \sqrt{\nu})}, \tag{21}$$

such that when $N > N_c^H$ then $H < 0$ and, therefore, the solution collapses at finite distance. We note that this condition makes sense only when $0 < N_H < \infty$, which implies $\rho < 1 + \sqrt{\nu}$. Conversely, when either $\rho \geq 1 + \sqrt{\nu}$ (no matter how large N) or $N \leq N_c^H$, then $H \geq 0$, in which case collapse is not guaranteed by the Virial Theorem.

Fig. 1 compares the critical power for collapse, N_c (17), the threshold-power N_c^H (21), and the “actual” power for collapse found from numerical simulations of the NLSM System (4), where the latter is obtained by gradually increasing the input power (or amplitude), i.e., N in the initial conditions (19), until the solution undergoes collapse. This figure also shows that for $\nu = 0.5$ and $-1 \leq \rho \leq 1$, N_c^H (21) is quite close to N_c , which, in turn, is very close to the numerically obtained threshold power for collapse in the NLSM System (4). For example, for the classical NLS (i.e., $\rho = 0$) the discrepancy between $N_c(R) \approx 1.86\pi$ and $N_c^H(R) = 2\pi$ is approximately 7% (see also [16]). In addition, in this entire parameter regime the discrepancy between N_c and the numerically-obtained threshold power is less than 2%. Furthermore, this figure shows that the change in the critical power with ρ is more pronounced for $\rho > 0$ than for $\rho < 0$. Similarly, Fig. 2 shows that for a wide range of the parameters, N_c^H (21) is a good approximation of N_c , which, in turn, is a good approximation of the numerically-obtained power for collapse. Furthermore, this figure shows that the critical power is weakly-dependent on ν , for either sign of ρ .

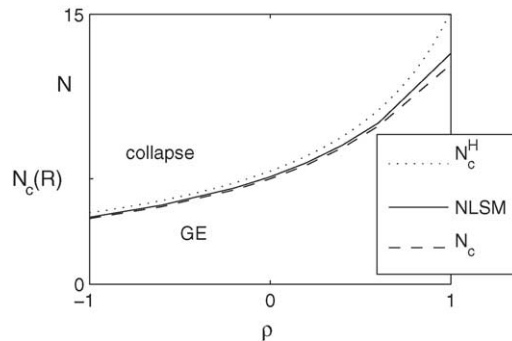


Fig. 1. The critical power for collapse as a function of ρ for $\nu = 0.5$ ($\rho < 0$ for water-waves and $\rho > 0$ for optics). N_c is obtained from the power of the ground-state [i.e., Eq. (17), dashes], N_c^H corresponds to $H = 0$ [i.e., Eq. (21), dotted], and the threshold power for collapse obtained by numerically integrating the NLSM [i.e., System (4) with (19), solid]. “GE” denotes global existence and “NLSM” denotes numerical simulations of System (4).

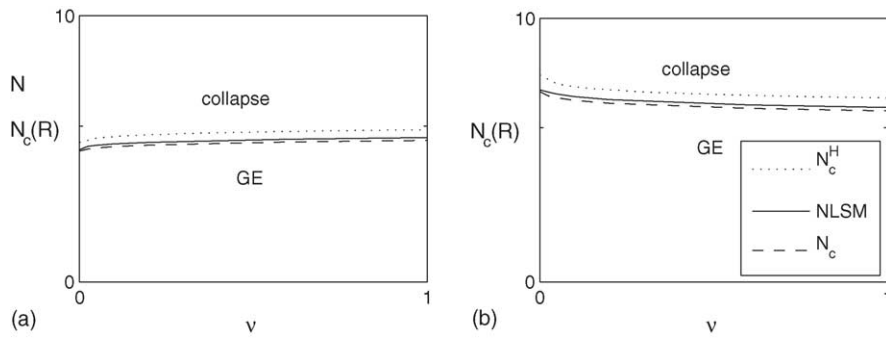


Fig. 2. Same as Fig. 1 with: (a) $\rho = -0.2$ and varying ν ; (b) $\rho = 0.2$ and varying ν .

An alternative way of using Eq. (20) is to fix N and allow ν and ρ to vary. Thus, for a fixed N there is a *separatrix curve* in the (ν, ρ) plane for which $H = 0$, given by

$$\rho_c^H(N, \nu) \equiv \left(1 - \frac{2\pi}{N}\right) (1 + \sqrt{\nu}), \tag{22}$$

such that when $\rho < \rho_c^H$ then $H < 0$ and collapse is guaranteed by the Virial Theorem. These separatrix curves are depicted in Fig 3, which is consistent in the case of $\rho > 0$ with the results of Crasovan et al. [12].

As discussed in Section 3, larger (more positive) values of ρ correspond to more defocusing. In fact, the results in this section show that when $\rho < 0$, or when $\rho > 0$ and sufficiently small, the defocusing effect induced by the coupling to the mean field is weaker than the focusing effect induced by the cubic term in Eq. (4a). In that case, collapse is guaranteed by the Virial Theorem for sufficiently large input power. On the other hand, when $\rho > 0$ and is sufficiently large, the defocusing effect induced by the coupling to the mean field can overcome the focusing effect induced by the cubic term in Eq. (4a). In that case, the NLSM can effectively behave as a defocusing NLS-type equation, i.e., like Eq. (1) with a negative sign before the cubic term.

We emphasize that $H \geq 0$ does not imply GE, because $H < 0$ is only a sufficient condition for collapse, not a necessary one. Nevertheless, owing to their explicitness and apparent accuracy, conditions (21) and (22) can be useful for predicting for the boundary in the (N, ν, ρ) space between the regions of collapse and GE. On the

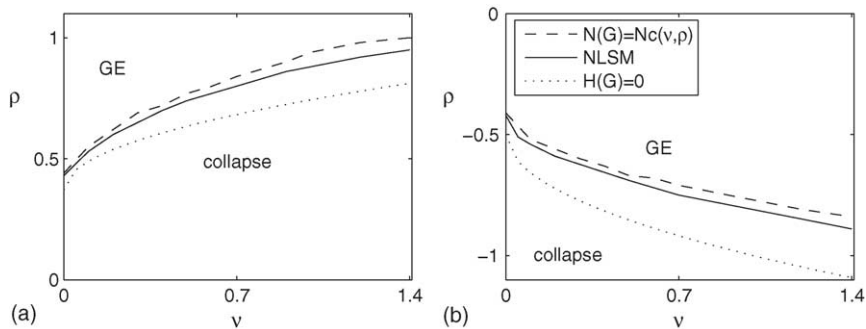


Fig. 3. The regions in the (ν, ρ) plane corresponding to collapse and global-existence (GE). Equating the power of the ground-state, $N_c(\nu, \rho)$ [i.e., Eq. (17)], to the power $N(G)$ of the initial conditions (19) [dashes, denoted by $N(G) = N(\nu, \rho)$ in the legend], ρ_c^H obtained from $H = 0$ [i.e., Eq. (22), dotted, denoted by $H(G) = 0$ in the legend], and using numerical simulations of the NLSM [i.e., System (4), solid] for: (a) nonlinear optics (i.e., $\rho > 0$) and the initial conditions (19) with the fixed input power $N(G) = 10$; (b) water waves (i.e., $\rho < 0$) and the initial conditions (19) with $N(G) = 4\pi/3$.

other hand, the condition derived from GE theory appears to be more accurate in the following sense: the actual (numerical) critical power appears to be slightly closer to N_c than to N_c^H . We note that in [16] a similar conclusion was reached for the NLS Eq. (1) when using Gaussian as well as other types of initial conditions.

4.1. Input astigmatism

It is interesting generalize the results above to the case when the initial conditions are astigmatic. To do that, consider the astigmatic Gaussian initial conditions

$$u_0^E(x, y) = \sqrt{\frac{2EN}{\pi}} e^{-[(Ex)^2+y^2]}, \tag{23}$$

where N is the input power and E is input ellipticity. Here $E = 1$ corresponds to radial symmetry, whereas $0 < E < 1$ and $E > 1$ correspond to relative elongation along the x and y axes, respectively.

Similar to Eq. (20), one arrives at (see Appendix B)

$$H(u_0^E, \phi_0^E) = \frac{1 + E^2}{2} N - \left(1 - \frac{\rho}{1 + \sqrt{v}/E}\right) \frac{EN^2}{2\pi}. \tag{24}$$

Thus, denoting

$$N_c^H(v, \rho, E) \equiv \frac{(E + 1/E)\pi}{1 - \rho/(1 + \sqrt{v}/E)}, \tag{25}$$

it follows that when $N > N_c^H$ then $H < 0$ and, therefore, the solution collapses at finite distance. This condition makes sense only when $0 < N_H < \infty$, which implies that $\rho < 1 + \sqrt{v}/E$.

Generally speaking, N_c^H increases with astigmatism. For example, let us consider the optics case with $0 < \rho < 1 + \sqrt{v}/E$ with an input beam (23) that is “focused” along the x direction, i.e., has $E > 1$. As E increases it will approach the value $E_c = \sqrt{v}/(\rho - 1)$, for which $N_c^H = \infty$. Physically speaking, this results suggests that as the input beam becomes narrower along the x -axis, the critical power for collapse increases, making the collapse more difficult to attain. This conclusion is consistent with the numerical observations of Crasovan et al. [12] in the optics case, and is in the same spirit as the results of Fibich and Ilan [17] for the NLS case (i.e., $\rho = 0$).

In addition, for a given power N , the separatrix curve in the (v, ρ) plane for which $H = 0$ is given by

$$\rho_c^H(N, v, E) \equiv \left[1 - \frac{(E + 1/E)\pi}{N}\right] \left(1 + \frac{\sqrt{v}}{E}\right), \tag{26}$$

such that when $\rho < \rho_c^H$ then $H < 0$ and, therefore, collapse is guaranteed by the Virial Theorem.

4.2. Related NLSM-type system

Consider the NLSM System (4) without the cubic term, i.e.,

$$iu_z + \frac{1}{2}\Delta u - \rho u\phi_x = 0, \tag{27a}$$

$$\phi_{xx} + v\phi_{yy} = (|u|^2)_x. \tag{27b}$$

One might expect that the nature of collapse in the NLSM-type System (27) would be similar to the NLSM System (4). Indeed, the analysis of System (27) is quite similar to that in Sections 3 and 4. The only difference is that the Hamiltonian corresponding to (27) is like (13), but without the second “self-focusing” integral, that is,

$$H(u, \phi) = \frac{1}{2} \int |\nabla u|^2 + \frac{\rho}{2} \int (\phi_x^2 + v\phi_y^2).$$

Since the Virial Theorem (14) remains unchanged, collapse is possible in System (27) whenever $\rho < 0$ and the initial conditions are sufficiently large. Furthermore, substituting the initial-conditions (19) into the Hamiltonian above gives

$$H(u_0, \phi_0) = N + \frac{\rho}{1 + \sqrt{\nu}} \frac{N^2}{2\pi}.$$

It follows that the threshold power for which $H = 0$ is given by

$$N_c^H(\nu, \rho) \equiv -\frac{2\pi(1 + \sqrt{\nu})}{\rho}.$$

Thus, similar to the NLSM case, the Virial Theorem guarantees that the solution of System (27) undergoes finite-distance collapse when $N > N_c^H$. To conclude, although the cubic term in the NLSM System (4) is self-focusing, its presence is not necessary for collapse to occur. In other words, collapse can occur even in the case when the nonlinearity is strictly and strongly nonlocal.

5. Astigmatic ground-states

Below we study how the astigmatism of the ground-state depends on ρ and ν . The astigmatism is recovered from the ground-state as

$$e(F) \equiv \frac{\int |(F^2)_x|}{\int |(F^2)_y|}. \tag{28}$$

It follows from (28) that $e = 1$ corresponds to a radially-symmetric ground-state, and $e < 1$ and $e > 1$ correspond to a ground-state that is relatively wider along the x and y axes, respectively. In other words, $e \approx L_y/L_x$, where L_x and L_y are the full-widths at half-max of the function.

Fig. 4(a) and (b) shows the on-axes amplitudes of the ground-state for $\rho = 0$ (i.e., the radially-symmetric R profile); $(\nu, \rho) = (0.5, -1)$; and $(\nu, \rho) = (0.5, 1)$. The contour plots in Fig. 4(c) and (d) correspond to the $\rho = -1$ and $\rho = 1$ cases, respectively. These plots clearly show that the ground-states with $\rho \neq 0$ are astigmatic. In addition, Fig. 5 shows the 3D plots and corresponding contour plots of the ground-state for $(\nu, \rho) = (4, -4)$, which has $e \approx 1.5$. Both $F(x, y)$ and the corresponding mean field $G(x, y)$ are clearly astigmatic. Furthermore, the mean field G is strongly nonlocal (see also Fig. 5d), as can be expected from the Poisson-type Eq. (15b) that it solves.

Fig. 6a shows that (i) the NLS ground-state ($\rho = 0$) is radially-symmetric, (i.e., $e = 1$); (ii) when $\nu = 0.5$ and $\rho < 0$ (water-waves) F is wider along the y -axis (i.e., $e > 1$); and (iii) when $\nu = 0.5$ and $\rho > 0$ (optics) F is wider along the x -axis (i.e., $e < 1$). We note that the parameter space explored in Figs. 1 and 6a is the same. Comparing these two figures, one sees that as ρ is changed from $\rho = 0$ (in either direction), the deviation from the NLS ground state is accompanied by a significant deviation in the critical power, as well as by a deviation from radial-symmetry. Therefore, as $|N_c(\nu, \rho) - N_c(\nu, 0)|$ increases with ρ , so does the astigmatism of the ground-state (along the x or y axes). On the other hand, Figs. 2 and 6b show that the critical power and the astigmatism are only weakly dependent on ν , for either sign of ρ . In addition, Fig. 6a shows that, for the same values of ν , the function F is relatively more astigmatic for $\rho > 0$ (i.e., for optics) than for $\rho < 0$ (i.e., for water waves).

In summary, one has the following *generic picture*:

- (1) The ground-state profile in the water-wave case is narrower along the direction of propagation (i.e., $e > 1$), whereas in the nonlinear optics case it is wider along the axis of linear polarization (i.e., $e < 1$).

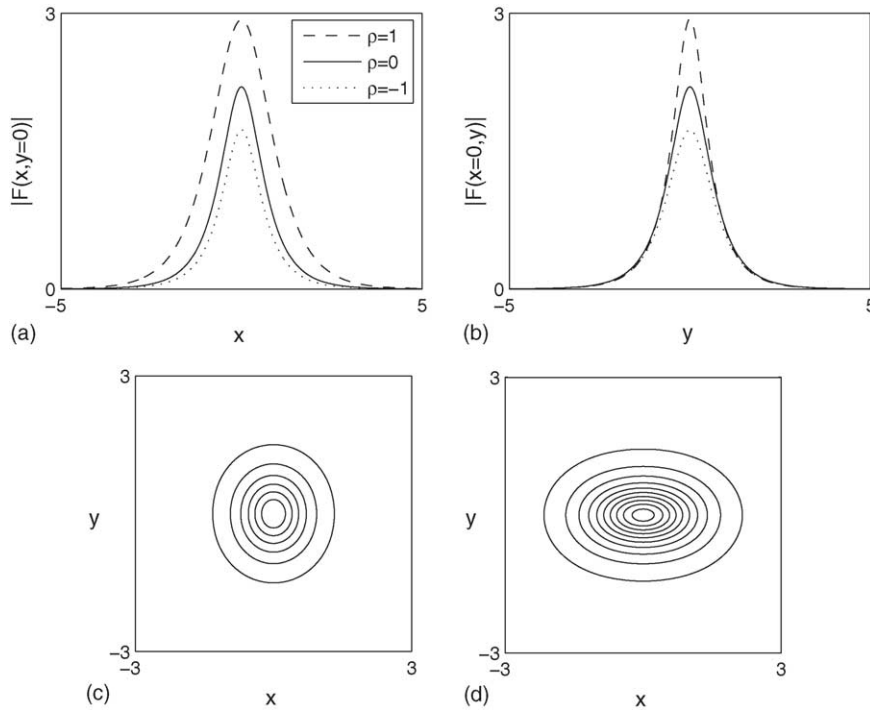


Fig. 4. Top: The on-axis amplitudes of the ground-state (a) along the y -axis and (b) along the x -axis for $(\nu, \rho) = (0.5, 1)$ (dashes), $\rho = 0$ (solid), and $(\nu, \rho) = (0.5, -1)$ (dotted). Bottom: Contour plots of $F(x, y)$ for: (c) $\rho = -1$ (corresponding to dotted above) with astigmatism [i.e., Eq. (28)] $e \approx 1.17$; (d) $\rho = 1$ (corresponding to dashes above) with $e \approx 0.59$.

- (2) The ground-state is relatively more astigmatic for nonlinear optics ($\rho > 0$) than for water waves ($\rho < 0$).
- (3) Whereas the astigmatism of the ground-state changes significantly with ρ , it depends only weakly on ν .

6. Quasi self-similar astigmatic collapse

Asymptotic analysis and numerical simulations strongly suggest that when collapse occurs in NLS Eq. (1), under quite general conditions, it occurs with a quasi self-similar profile that is a modulation (up to a phase) of the ground-state (cf. [30]), i.e.,

$$|u(x, y, z)| \sim \frac{1}{L(z)} R\left(\frac{r}{L(z)}\right), \quad (29)$$

where (x, y) are in some region surrounding of the collapse point (which typically shrinks during the self-focusing process), $R(r)$ is the NLS ground-state (see Section 3), and $L(z)$ is a modulation function, such that $\lim_{z \rightarrow Z_c} L(z) = 0$, where Z_c is the collapse distance (or time). In the NLS case, the ground-state $R(r)$ is radially-symmetric and, to the best of our knowledge, all the NLS-collapse simulations to date have shown that collapse occurs with a radially-symmetric profile. The quasi self-similar collapse has received much theoretical attention since the contribution of Merle and Tsutsumi [25]. However, it is very difficult to justify (29) rigorously. Only very recently did Merle and Raphael [26] provide a sharp result explaining this quasi self-similar behavior in the case of the NLS Eq. (1). Furthermore, on the experimental side, Gaeta and coworkers [24] recently carried out detailed measurements in optical Kerr media showing that the collapse process occurs with a self-similar profile, in consistency with Eq. (29).

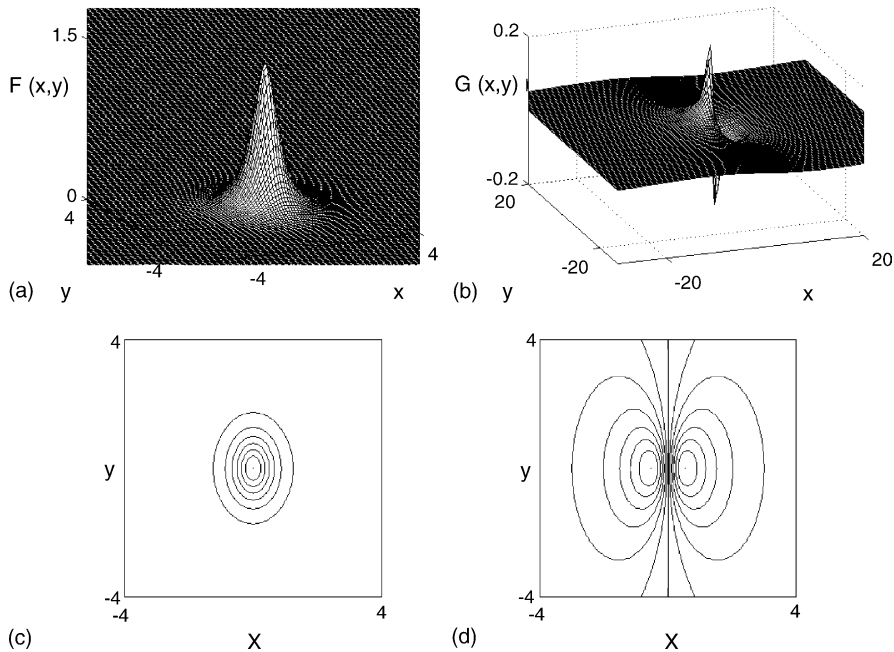


Fig. 5. The ground-state [i.e., solution of System (15)] for $(v, \rho) = (4, -4)$. (a) and (b) are 3D plot of $F(x, y)$ and $G(x, y)$, respectively; (c) and (d) are contour plots corresponding to (a) and (b), respectively.

In contrast to the NLS case, when $\rho \neq 0$ and $v > 0$ the NLSM System (4) is not rotationally invariant and the stationary solutions of (15) are not radially symmetric. Moreover, with this choice of parameters the stationary solutions cannot be transformed into radially-symmetric functions by any rescaling of x and y . Therefore, the NLSM ground-state, $F(x, y)$, is inherently astigmatic, which makes the analysis and numerical simulations more difficult. The asymptotic analysis of Papanicolaou et al. [28] indicates that, similar to the NLS collapse, NLSM collapse occurs with a modulated profile, i.e.,

$$|u(x, y, z)| \sim \frac{1}{L(z)} P\left(\frac{x}{L(z)}, \frac{y}{L(z)}, b(z)\right), \tag{30}$$

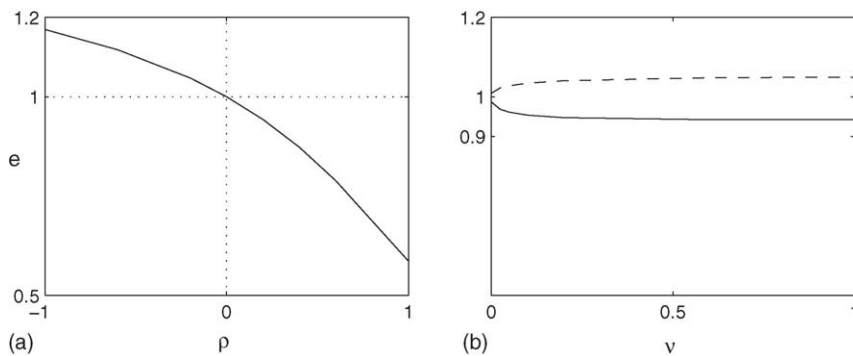


Fig. 6. The astigmatism (28) of the ground-state $F(x, y)$ of System (4) for: (a) $v = 0.5$ with $-1 \leq \rho \leq 1$ (i.e., same as Fig. 1); (b) $\rho = -0.2$ (dashes) and $\rho = 0.2$ (solid) with $0 \leq v \leq 1$ (i.e., same as Fig. 2a and b, respectively).

for certain functions $P(x, y, z)$, $L(z)$, and $b(z)$, such that as $z \rightarrow Z_c$, $L(z)$ and $b(z)$ approach zero and $P(x, y, z)$ asymptotically approaches the corresponding ground-state $F(x, y)$. Numerical simulations of the NLSM using “dynamic rescaling” suggested that, indeed, the collapsing solution approaches a modulated profile. However, in [28] the ground-state itself was not computed. Since it was not computed, it was not shown (numerically) that the asymptotic profile approaches the corresponding ground-state. The numerical results in this section suggest that, down to moderately small values of $L(z)$, the amplitude of the collapsing solution behaves as

$$|u(x, y, z)| \sim \frac{1}{L(z)} F\left(\frac{x}{L(z)}, \frac{y}{L(z)}\right), \tag{31}$$

where $F(x, y)$ is the ground-state of System (4). Therefore, the results of this study strengthen those of [28], because the collapsing wave is directly compared to the corresponding ground-state and is shown to approach a quasi self-similar modulation of the ground-state itself.

To study NLSM collapse numerically, System (4) is solved with the Gaussian initial conditions (19). The self-focusing dynamics are recovered from the simulations using the focusing factor, $|u(0, 0, z)|/u_0(0, 0)$, as a function of the propagation distance z . The astigmatism of the solution is recovered in accordance with (28) as

$$e(z) = \frac{\int |(|u|^2)_x|}{\int |(|u|^2)_y|}. \tag{32}$$

We begin by presenting several numerical simulations of collapse, that also serve to verify some of the results of the previous sections. As noted in Section 3, the Hamiltonian of the NLSM suggests, loosely speaking, that the water-wave case ($\rho < 0$) is “more focusing” than the optics case ($\rho > 0$). Indeed, Fig. 7 shows that when the same initial conditions are used for all cases, collapse with $\rho = -1$ precedes collapse with $\rho = 0$, which, in turn precedes collapse with $\rho = 1$. For this figure, the input power is taken as $1.2N_c(\nu = 0.5, \rho = 1) \approx 12.2$. We note that this value of N_c is approximately twice as large as $N_c(R)$ and approximately 3.3 times larger than $N_c(\nu = 0.5, \rho = -1)$ (see Fig. 1).

Since $\rho < 0$ and $\rho > 0$ correspond water waves and optics, respectively, and since critical power depends on ρ , a more “balanced” comparison between the water-wave and optics cases requires using the same initial conditions with an input power chosen with respect to the corresponding critical power (which is different for water-waves and optics). Therefore, the rest of the simulations below [i.e., Figs. 8–13] use the input power $N = 1.2N_c(\nu, \rho)$, i.e., 20% above the corresponding critical power for collapse. Fig. 8a shows the dynamics of the focusing factor for $\nu = 0.5$ with: $\rho = 0$ (NLS), $\rho = 1$ (optics), and $\rho = -1$ (water waves). Similarly to Fig. 7, the collapse distance with $\rho > 0$ is greater than with $\rho \leq 0$. Surprisingly, the collapse distance in the $\rho = 0$ and $\rho < 0$ cases is almost the

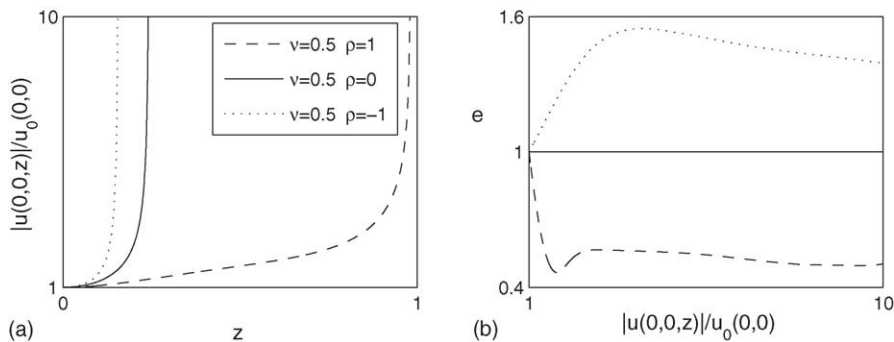


Fig. 7. (a) The focusing factor the NLSM solutions [i.e., System (4)] with $\nu = 0.5$ and three values of ρ (see legend) using the initial conditions (19) with the same input power $N = 1.2N_c(\nu = 0.5, \rho = -1) \approx 12.2$. (b) The corresponding astigmatism (32) of the solution as a function of the focusing factor.

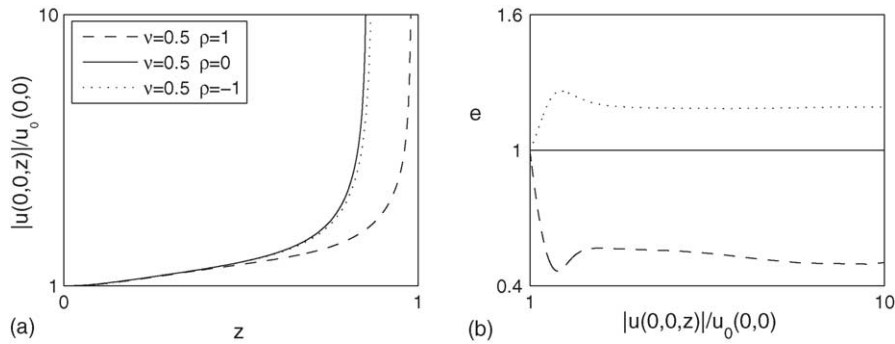


Fig. 8. Same as Fig. 7, but with the input power $N = 1.2N_c(v, \rho)$, i.e., 20% above the corresponding critical power.

same. Although one might have expected the collapse with $\rho < 0$ to precede collapse with $\rho = 0$ (as in Fig. 7), this is not the case here, because $N(\rho = -1)$ is approximately 1.6 times smaller than $N(\rho = 0)$ (see Fig. 3). Thus, in Fig. 8 the collapse distances of the $\rho = -1$ and $\rho = 0$ simulations are close, because the input power in the $\rho = 0$ simulation is much larger than the input power in the $\rho = -1$ one.

In addition, Fig. 8b shows the corresponding astigmatism plots. The astigmatism is plotted as a function of the focusing factor (rather than as a function of z) in order to “blow up” the dynamics near the collapse point, where the interesting changes in the astigmatism are expected to occur. While the NLS solution remains radially-symmetric (i.e., $e \equiv 1$), the NLSM solutions become astigmatic during propagation. Furthermore, $\rho < 0$ and $\rho > 0$ correspond

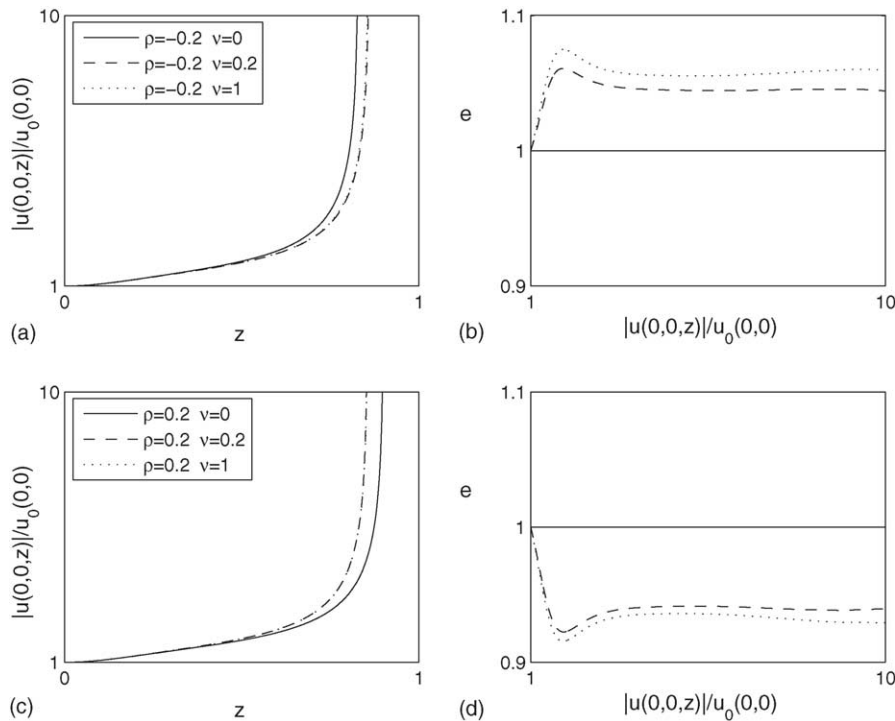


Fig. 9. Same as Fig. 8 with [(a) and (b)] $\rho = -0.2$ and $v = 0$ (solid), $v = 0.2$ (dashes), and $v = 1$ (dotted, on top of the dashes); [(c) and (d)] same as above with $\rho = 0.2$.

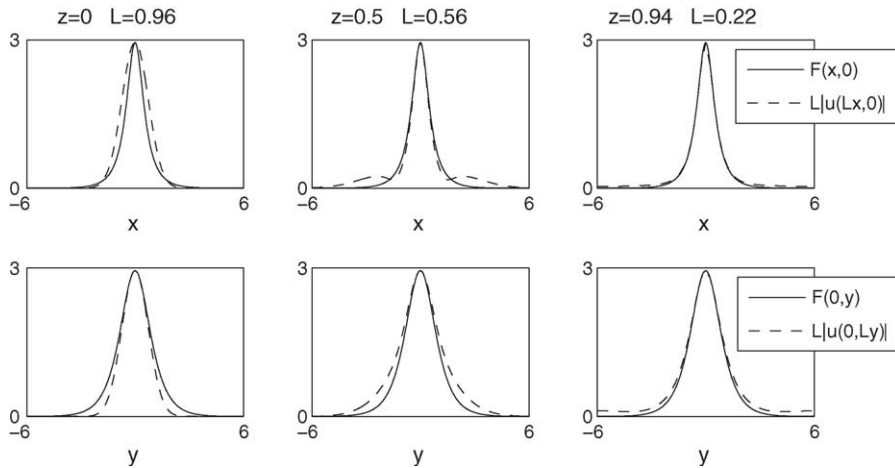


Fig. 10. Convergence of the modulated collapse profile (dashes) to the NLSM ground state (solid) along the x -axis (top) and the y -axis (bottom) with $(\nu, \rho) = (0.5, 1)$. The initial conditions are (19) with $N = 1.2N_c(\nu, \rho)$.

to $e > 1$ and $e < 1$, respectively, which is consistent with in Figs. 4 and 6. As can be seen from this figure, at the initial stage of the propagation the astigmatism of the NLSM solutions becomes large, in a direction that depends on ρ . Based on these simulations it appears that the astigmatism approaches a (more or less) constant value at the collapse point, a value that depends on ν and ρ (such that $e \neq 1$). This is consistent with the results in [28], as well as with the results presented below.

Figs. 7–9 indicate that NLSM collapse is astigmatic, however, they do not show that the collapse process is quasi self-similar. In order to study the self-similarity of the collapse process, in accordance with Eq. (31), the modulation function is recovered from the solution as

$$L(z) = \frac{F(0, 0)}{|u(0, 0, z)|},$$

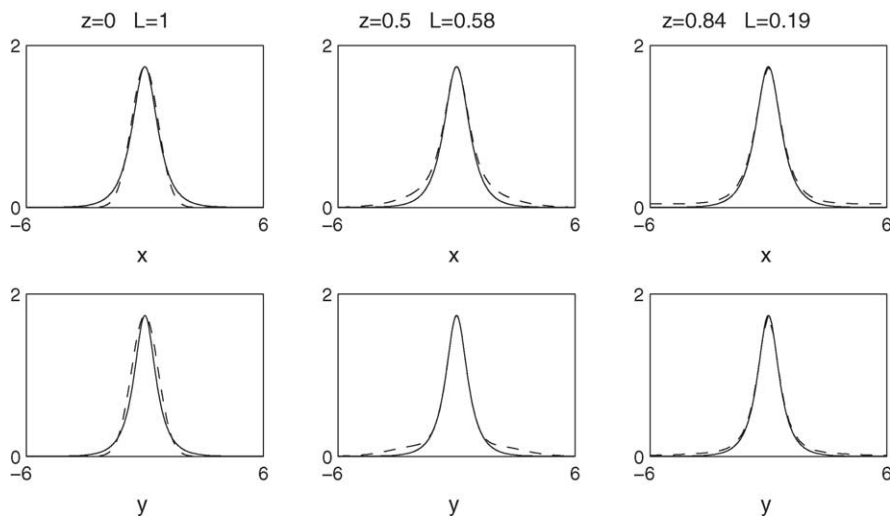


Fig. 11. Same as Fig. 10 with $(\nu, \rho) = (0.5, -1)$.

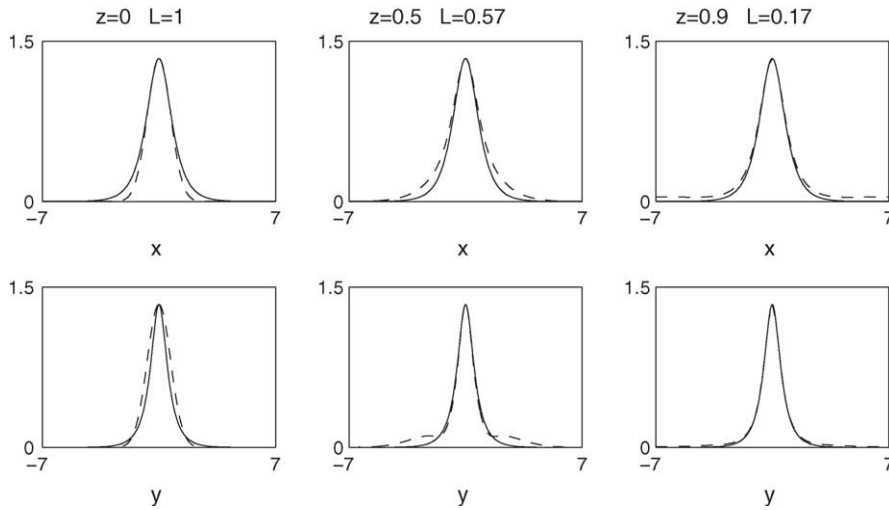


Fig. 12. Same as Fig. 10 with $(v, \rho) = (4, -4)$.

where $F(x, y)$ is the corresponding ground-state. The rescaled amplitude of the solution of the NLSM, i.e., $L|u(L\tilde{x}, L\tilde{y}, z)|$, is compared with $F(\tilde{x}, \tilde{y})$, where $F(\tilde{x}, \tilde{y})$ is the ground-state and $(\tilde{x}, \tilde{y}) = (\frac{x}{L}, \frac{y}{L})$. In order to show that the collapse process is, indeed, quasi self-similar with the corresponding ground-state, the rescaled amplitude is shown to converge pointwise to F near the origin as $z \rightarrow Z_c$ (i.e., near the collapse point).

Fig. 10 shows that the NLSM collapse is indeed self-similar with the ground-state for $v = 0.5$ and $\rho = 1$. The rescaled on-axis amplitude is compared separately on the x and y axes (top and bottom plots, respectively). One can see that, as the solution is undergoing self-focusing [i.e., as $L(z)$ approached zero], its rescaled profile approaches that of the astigmatic ground-state near the origin.

Fig. 11 shows the same picture with $\rho = -1$, whose ground-state is somewhat less astigmatic than with $\rho = 1$ (as mentioned above). In order to observe self-similar collapse with $\rho < 0$ and a more astigmatic profile, Fig. 12

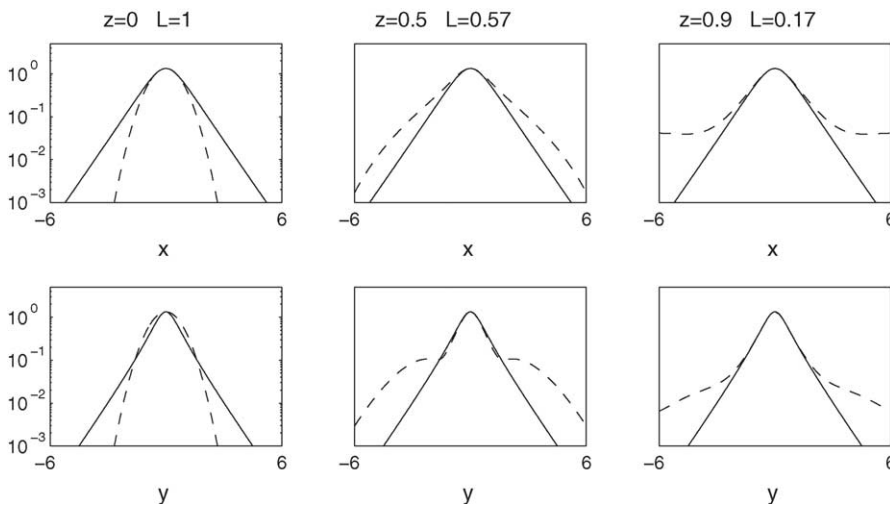


Fig. 13. Same as Fig. 12 on a semi-log plot.

compares the solution and the ground-state with $\nu = 4$ and $\rho = -4$. The ground-state in this latter case is clearly astigmatic and, in turn, the collapse process is quasi self-similar with the ground-state. Fig. 13 further demonstrates the local nature of the self-similar collapse process. While the spatial region in the vicinity of the collapse point is self-similar to the ground-state, the outer “wings” of the solution do not approach the ground-state. This phenomenon is well-known in the NLS case as well [30], and can be understood as follows: in accordance with Eq. (31), exactly one critical power enters the collapse region. More precisely, as $z \rightarrow Z_c$, the power of $u(x, y, z)$ contained in a “ball” of radius $L(z)$ around the collapse point is just slightly above N_c (cf. [25]). Since the input power is 20% above N_c , the residual 20% radiates into the outer wings in a process that is not self-similar with the ground-state.

7. Collapse arrest

As mentioned in Section 2.2, within the context of nonlinear optics, the self-focusing mechanism in the NLSM is due to a quadratic effect [1,2]. However, it is well-known that collapse with an infinite amplitude does not occur in physical situations. In reality, there are always physical mechanisms that arrest the collapse. Such mechanisms have been studied extensively in nonlinear optics, e.g., nonlinear saturation [11,33], beam nonparaxiality [15], and vectorial effects [18]. In order to investigate the arrest of collapse in NLSM in the optics case, we consider the NLSM with a small nonlinear saturation of the cubic nonlinearity as

$$iu_z + \frac{1}{2}\Delta u + \frac{|u|^2 u - \rho u \phi_x}{1 + \varepsilon|u|^2} = 0, \quad (33a)$$

$$\phi_{xx} + \nu\phi_{yy} = (|u|^2)_x, \quad (33b)$$

where ε is the small nonlinear-saturation parameter.

When $\rho \ll 1$ and $\varepsilon \ll 1$ System (33) is a small perturbation of the NLS Eq. (1). In that case, the asymptotic analysis of Fibich and Papanicolaou [19] for the perturbed NLS can be used. Their analysis is based on the asymptotic and numerical observations that the collapsing solution in the NLS case is self-similar with the ground-state (Townes profile), i.e., as in Eq. (29). The asymptotic analysis predicts that, to leading order, the dynamics of the focusing factor in the solution of System (33) is given by the following ODE (see [19, 5.3–5.4])

$$(w_z)^2 = -\frac{4H_0}{M} \frac{(w_M - w)(w - w_m)}{w}, \quad (34)$$

where $w(z) = L^2(z)$, $L(z)$ is the focusing-factor in Eq. (29), $M \approx 0.55$, and H_0 , w_M , and w_m are constants that depend only on ε and the initial conditions, such that $w_M > w_m$. It follows from this nonlinear-oscillator-type equation that for generic initial conditions the intensity of the solution initially focuses [i.e., $L(z)$ decreases] until $L \sim \sqrt{w_m} = O(\sqrt{\varepsilon})$, then defocuses [i.e., $L(z)$ increases] until $L \sim \sqrt{w_M}$, followed by focusing–defocusing oscillations, such that $\sqrt{w_m} \leq L(z) \leq \sqrt{w_M}$.

Fig. 14 shows the on-axis amplitude of the numerical solution of System (33) for $\rho = 0.5$, $\nu = 1$, $\varepsilon = 0.0025$, and the initial conditions (19) with $N = 1.5N_c$, where N_c is the critical power corresponding to $\varepsilon = 0$. The numerical solution of System (33) agrees qualitatively with the predictions based on Eq. (34). Indeed, one sees that collapse is arrested by the small nonlinear saturation, followed by a series of focusing–defocusing oscillations.

It should be mentioned that the physical mechanisms that arrest the collapse in water waves are not understood to the same level as in optics, in part because of the scarce experimental results on water waves with large surface tension.

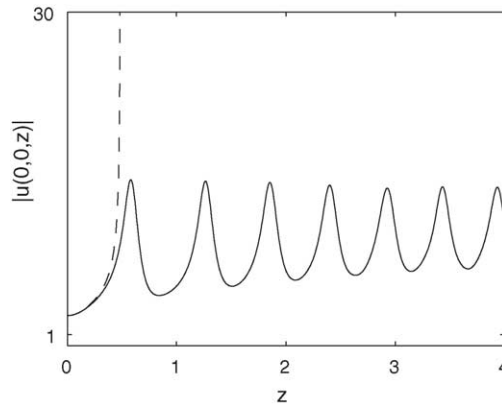


Fig. 14. Collapse in the NLSM [i.e., System (4) with $(\nu, \rho) = (1, 0.5)$, dashes] is arrested by small nonlinear saturation [i.e., System (33) with $(\nu, \rho) = (1, 0.5)$ and $\varepsilon = 0.0025$, solid] leading instead to focusing–defocusing oscillations.

8. Summary and final remarks

The results of this study show that nonlinear-wave systems that admit a quadratic–cubic type interaction, such as in nonlinear optics and in nonlinear free-surface water waves, lead to the NLSM System (4). The NLSM can admit finite-distance collapse in a certain parameter regime. The regions of collapse and global-existence is explored in a relevant parameter space and the consistency between global existence theory, the Virial Theorem, and numerical simulations the NLSM System (4) is established. Furthermore, numerical simulations of the NLSM show that the collapse process occurs with a quasi self-similar profile, which is a modulation of the ground-state profile. The ground-state profile is found using a numerical algorithm that was recently used in dispersion-managed NLS theory. Generically, the ground-state profile is astigmatic and, therefore, the collapse profile is astigmatic as well.

These results are in the same spirit as for the NLS Eq. (1). However, NLSM theory is more difficult and not as advanced as NLS theory. There are several remaining questions and problems. For example, it remains an open problem to extend the sharp theoretical results on the self-similar nature of the singularity to the NLSM case. From the numerical perspective, while our simulations indicate that NLSM collapse occurs with a self-similar ground-state, we only resolve moderate focusing factors [i.e., $O(10)$] near the collapse point. Using more specialized numerical methods (cf. [28,20]), much larger focusing factors (e.g., greater than 10^4) could furnish more convincing evidence of this self-similar collapse. From the experimental perspective, self-similar collapse in quadratic–cubic type media remains to be demonstrated in either free-surface water waves or nonlinear optics.

Acknowledgments

This research was partially supported by the U.S. Air Force Office of Scientific Research, under grant 1-49620-03-1-0250 and by the National Science Foundation, under grant DMS-0303756.

Appendix A. Proof of Proposition 3.2

Following Weinstein [35], if one substitutes the stationary solution (15) into the Virial Theorem (14), one finds that the variance, i.e., the integral on left-hand side, is independent of z . Therefore, its second- z derivative is zero, which implies that the right-hand side, i.e., the Hamiltonian of the stationary solution (15), is zero as well. \square

Below an alternative constructive proof is given. Multiplying Eq. (15a) by F and Eq. (15b) by G and integrating gives

$$-\lambda \int F^2 + \frac{1}{2} \int (FF_{xx} + FF_{yy}) + \int F^4 - \rho \int F^2 G_x = 0, \quad (\text{A.1a})$$

$$\int (GG_{xx} + \nu GG_{yy}) = \int (F^2)_x G. \quad (\text{A.1b})$$

Using integration by-parts (IBP) on (A.1b) gives

$$\int F^2 G_x = \int (\nabla_\nu G)^2, \quad (\text{A.2})$$

where $(\nabla_\nu G)^2 \equiv G_x^2 + \nu G_y^2$. Combining (A.1b) and (A.1a) leads to

$$\lambda \int F^2 + \frac{1}{2} \int (\nabla F)^2 - \int F^4 + \rho \int (\nabla_\nu G)^2 = 0. \quad (\text{A.3})$$

On the other hand, multiplying Eq. (15a) by $(xF_x + yF_y)$ gives that

$$\begin{aligned} & -\frac{\lambda}{2} \int [x(F^2)_x + y(F^2)_y] + \frac{1}{4} \int [x(F_x^2)_x + y(F_y^2)_y] + \frac{1}{2} \int (xF_{yy}F_x + yF_{xx}F_y) \\ & + \frac{1}{4} \int [x(F^4)_x + y(F^4)_y] - \frac{\rho}{2} \int [x(F^2)_x G_x + y(F^2)_y G_x] = 0. \end{aligned}$$

Using IBP several times on the first four terms we arrive at

$$\lambda \int F^2 - \frac{1}{2} \int F^4 - \frac{\rho}{2} \int [x(F^2)_x G_x + y(F^2)_y G_x] = 0. \quad (\text{A.4})$$

Similarly, multiplying Eq. (A.1b) by $(xG_x + yG_y)$ and using IBP leads to

$$\int [x(F^2)_x G_x + y(F^2)_y G_y] = 0.$$

Using IBP and Eq. (A.2) gives

$$\int [x(F^2)_x G_x + y(F^2)_y G_x] = - \int F^2 G_x = - \int (\nabla_\nu G)^2. \quad (\text{A.5})$$

Substituting (A.5) into (A.4) we obtain that

$$\lambda \int F^2 - \frac{1}{2} \int F^4 + \frac{\rho}{2} \int (\nabla_\nu G)^2 = 0.$$

Subtracting from Eq. (A.3) gives Eq. (18). \square

Appendix B. Derivation of the Hamiltonians (20) and (24)

The derivation of Eq. (24) is outlined below. Substituting the astigmatic Gaussian initial conditions (23) into the first two terms of the Hamiltonian (13) gives

$$\frac{1}{2} \int |\nabla u_0|^2 - \frac{1}{2} \int |u_0|^4 = \frac{(1 + E^2)N}{2} - \frac{EN^2}{2\pi}. \quad (\text{B.1})$$

It remains to calculate the third term in Eq. (13). To do that it is convenient to use the Fourier Transform. Below we denote

$$\hat{f}(k_x, k_y) = \mathcal{F}[f] \equiv \int f(x, y) e^{-ik_x x - ik_y y}, \quad f(x, y) = \mathcal{F}^{-1}[\hat{f}] \equiv \frac{1}{(2\pi)^2} \int \hat{f}(k_x, k_y) e^{ik_x x + ik_y y},$$

as the direct and inverse 2D Fourier Transforms, respectively, where (k_x, k_y) are the Fourier frequencies in (x, y) directions and the integrations are carried over the (x, y) and (k_x, k_y) planes, respectively. Therefore, it follows from Eq. (4b) that

$$\hat{\phi}_0 \equiv \mathcal{F}[\phi(x, y, 0)] = -\frac{ik_x}{k_x^2 + vk_y^2} \hat{u}_0^2.$$

Using Parseval's identity and substituting the Gaussian initial conditions (19) leads to

$$\int (\phi_x^2 + v\phi_y^2) = \frac{1}{4\pi^2} \int \frac{k_x^2 (\hat{u}_0^2)^2}{k_x^2 + vk_y^2} = \frac{N^2}{4\pi^2} \int \frac{k_x^2 e^{-(k_x^2 + E^2 k_y^2)/(4E^2)}}{k_x^2 + vk_y^2}.$$

Transforming to the cylindrical coordinates defined by $(k_x, k_y) = (r \cos \theta, E^{-1} r \sin \theta)$ yields

$$\frac{\rho}{2} \int (\phi_x^2 + v\phi_y^2) = \frac{\rho N^2}{8\pi^2 E} \int_0^\infty e^{-r^2/4E^2} r \, dr \int_0^{2\pi} \frac{d\theta}{1 + (v/E^2) \cot^2 \theta} = \frac{\rho N^2 E}{4\pi^2} \frac{2\pi}{1 + \sqrt{v}/E}.$$

Combining with Eq. (B.1) and the Hamiltonian (13) yields Eq. (24). Note that Eq. (20) is a special case of Eq. (24) with $E = 1$.

Appendix C. Calculating the ground state

The NLSM ground state is obtained in this study using a fixed-point numerical procedure similar to that recently used in dispersion-managed soliton theory (cf. [5,29]).

Below we use the following formulation. Let $u(x, y, z)$ and $v(x, y, z)$ be solutions of the system

$$iu_z + \frac{1}{2}(u_{xx} + u_{yy}) + |u|^2 u - \rho u v = 0, \quad (\text{C.1a})$$

$$v_{xx} + v v_{yy} = (|u|^2)_{xx}. \quad (\text{C.1b})$$

We note that Systems (4) and (C.1) are mathematically equivalent under the transformation $v \equiv \phi_x$. A stationary solution of system (C.1) has the form $u(x, y, z) = e^{i\lambda z} F(x, y)$ and $v(x, y, z) = V(x, y)$, where F and V are real functions and λ is an arbitrary real number. Substituting this ansatz into system (C.1) gives

$$-\lambda F + \frac{1}{2}(F_{xx} + F_{yy}) + F^3 - \rho F V = 0, \quad (\text{C.2a})$$

$$V_{xx} + v V_{yy} = (F^2)_{xx}. \quad (\text{C.2b})$$

When the stationary solutions are known to be radially-symmetric, e.g., when $\rho = 0$ or $v = 0$, one can write this system as a single ODE in the radial variable. In that case, one can solve the ODE using a “shooting” method. This technique, however, does not work well for a “true” PDE, i.e., when F and G are not radially-symmetric, which is the case in this study when both ρ and v are nonzero. Therefore, in order to solve this system we use a fixed-point method as explained below.

Taking the Fourier Transform (see [Appendix B](#)) of System (C.2) gives

$$-\lambda \hat{F} - \frac{|k|^2}{2} \hat{F} + \mathcal{F}[F^3 - \rho FV] = 0, \quad (k_x^2 + \nu k_y^2) \hat{V} = k_x^2 \mathcal{F}[F^2],$$

where $\hat{F}(k_x, k_y)$ and $\hat{V}(k_x, k_y)$ are the Fourier transforms of $F(x, y)$ and $V(x, y)$, respectively, and $|k|^2 = k_x^2 + k_y^2$. This system can be re-written as

$$\hat{F} = \frac{1}{\lambda + |k|^2/2} \mathcal{F}[F^3 - \rho FV], \quad (\text{C.3a})$$

$$\hat{V} = \frac{k_x^2}{k_x^2 + \nu k_y^2} \mathcal{F}[F^2]. \quad (\text{C.3b})$$

The idea is to use the fixed-point iterative method

$$\hat{F}^{(n+1)} = \frac{1}{\lambda + |k|^2/2} \mathcal{F}[F^3 - \rho FV]^{(n)},$$

where the right-hand side is evaluated using $V^{(n)}$ found using Eq. (C.3b). This procedure is then supplemented with an initial guess $F^{(0)}(x, y) = f_0(x, y)$, which is typically chosen to be a Gaussian, i.e., $f_0(x, y) = e^{-x^2 - y^2}$. However, this approach fails, because the right-hand side of Eq. (C.2) is nonlinear and, as a result, the iterations either converge to the trivial solution or diverge to infinity. To rectify this problem, one can “homogenize” the right-hand side of Eq. (C.3) as follows. Multiplying (C.3a) by \hat{F}^* and integrating over the (k_x, k_y) plane yields the equation $\text{SL} = \text{SR}$, where

$$\text{SL} \equiv \int |\hat{F}|^2, \quad \text{SR} \equiv \int \frac{1}{\lambda + |k|^2/2} \mathcal{F}[F^3 - \rho FV] \hat{F}^*.$$

Here SL and SR are two scalar quantities that can be efficiently calculated using Fast-Fourier Transforms. Since $\text{SL} = \text{SR}$ when F and V are solutions of (C.2), one can use instead the modified iterative method

$$\hat{F}^{(n+1)} = \frac{1}{\lambda + |k|^2/2} \left(\frac{\text{SL}}{\text{SR}} \right)^\alpha \mathcal{F}[F^3 - \rho FV]^{(n)}, \quad (\text{C.4})$$

where SL and SR are calculated using F and V at step n and $V^{(n)}$ is found using Eq. (C.3b). Here α is an arbitrary constant that is chosen to make the right-hand side of (C.4) have homogeneity zero with respect to F , which is to be expected to prevent the aforementioned divergence. In our case the right-hand side of (C.4) scales like $(\text{SL}/\text{SR})^\alpha F^3 = F^{3-2\alpha}$. This observation suggests using $\alpha = 3/2$, which, indeed, allows the fixed-point method (C.4) to converge. The convergence can be monitored using error := $|(\text{SL}/\text{SR}) - 1|$, which should approach zero. Typically, 20–40 steps suffice for obtaining error $< 10^{-8}$. In addition, when the solution obtained by this method is substituted for the initial conditions of the NLSM System (4), the NLSM solution is confirmed to be stationary, i.e., its amplitude remains (approximately) constant for a propagation distance of $z = \text{O}(10)$.

References

- [1] M.J. Ablowitz, G. Biondini, S. Blair, Multi-dimensional pulse propagation in resonant materials $\chi^{(2)}$ materials, *Phys. Lett. A* 236 (1997) 520.
- [2] M.J. Ablowitz, G. Biondini, S. Blair, Nonlinear Schrödinger equations with mean terms in nonresonant multidimensional quadratic materials, *Phys. Rev. E* 63 (2001) 605.

- [3] M.J. Ablowitz, P.A. Clarkson, *Solitons, Nonlinear Evolution Equations and Inverse Scattering*, Cambridge University Press, Cambridge, 1991.
- [4] M.J. Ablowitz, R. Haberman, Nonlinear evolution equations—two three dimensions, *Phys. Rev. Lett.* 35 (1975) 1185.
- [5] M.J. Ablowitz, Z. Musslimani, Dark and gray strongly-dispersion managed solitons, *Phys. Rev. E* 67 (2003) 025601(R).
- [6] M.J. Ablowitz, H. Segur, On the evolution of packets of water waves, *J. Fluid Mech.* 92 (1979) 691.
- [7] M.J. Ablowitz, H. Segur, *Solitons and the Inverse Scattering Transform*, SIAM, Philadelphia, 1981.
- [8] D.J. Benney, G.J. Roskes, Wave instabilities, *Stud. Appl. Math.* 48 (1969) 377.
- [9] R.Y. Chiao, E. Garmire, C.H. Townes, Self-trapping of optical beams, *Phys. Rev. Lett.* 13 (1964) 479.
- [10] R. Cipolatti, On the existence of standing waves for the Davey–Stewartson system, *Commun. Part. Diff. Eq.* (1992) 967.
- [11] B.I. Cohen, B.F. Lasinski, A.B. Langdon, J.C. Cummings, Dynamics of ponderomotive self-focusing in plasmas, *Phys. Fluids B-Plasma Phys.* 3 (1992) 766.
- [12] L.C. Cravosan, J.P. Torres, D. Mihalache, L. Torner, Arresting wave collapse by self-rectification, *Phys. Rev. Lett.* 91 (2003) 063904.
- [13] A. Davey, K. Stewartson, On three-dimensional packets of surface waves, *Proc. R. Soc. Lond. A* 338 (1974) 101.
- [14] V.D. Djordevic, L.G. Reddekopp, On two-dimensional packets of capillary gravity waves, *J. Fluid Mech.* 79 (1977) 703.
- [15] G. Fibich, Small beam nonparaxiality arrests self-focusing of optical beams, *Phys. Rev. Lett.* 76 (1996) 4356.
- [16] G. Fibich, A.L. Gaeta, Critical power for self-focusing in bulk media and in hollow waveguides, *Opt. Lett.* 25 (2000) 335.
- [17] G. Fibich, B. Ilan, Self-focusing of elliptic beams: an example for the failure of the aberrationless approximation, *J. Opt. Soc. Am. B* 17 (2000) 1749.
- [18] G. Fibich, B. Ilan, Vectorial and random effects in self-focusing and in multiple filamentation, *Physica D* 157 (2001) 113.
- [19] G. Fibich, G.C. Papanicolaou, Self-focusing in the perturbed and unperturbed nonlinear Schrödinger equation in critical dimension, *SIAM J. Appl. Math.* 60 (1999) 183.
- [20] G. Fibich, W. Ren, X.P. Wang, Numerical simulations of self-focusing of ultrafast laser pulses, *Phys. Rev. E* 67 (2003) 056603.
- [21] A.S. Fokas, M.J. Ablowitz, On a method of solution for a class of multidimensional nonlinear evolution equations, *Phys. Rev. Lett.* 51 (1983) 7.
- [22] J.M. Ghidaglia, J.C. Saut, On the initial value problem for the Davey–Stewartson systems, *Nonlinearity* 3 (1990) 475.
- [23] P.L. Kelley, Self focusing of optical beams, *Phys. Rev. Lett.* 15 (1965) 1005.
- [24] K.D. Moll, A.L. Gaeta, G. Fibich, Self-similar optical wave collapse: observation of the Townes profile, *Phys. Rev. Lett.* 90 (2003) 203902.
- [25] F. Merle, Y. Tsutsumi, L^2 concentration of blow-up solutions for the nonlinear Schrödinger equation with critical power nonlinearity, *J. Diff. Eq.* 84 (1990) 205.
- [26] F. Merle, P. Raphael, On the universality of blow-up profile for L^2 critical nonlinear Schrödinger equation, *Inventiones Mathematicae* 156 (2004) 565.
- [27] G.C. Papanicolaou, D. McLaughlin, M. Weinstein, Focusing singularity for the nonlinear Schrödinger equation, *Lec. No. Numer. Appl. Anal.* 5 (1982) 253.
- [28] G.C. Papanicolaou, C. Sulem, P.L. Sulem, X.P. Wang, The focusing singularity of the Davey–Stewartson equations for gravity-capillary surface waves, *Physica D* 72 (1994) 61.
- [29] V.I. Petviashvili, Equation of an extraordinary soliton, *Sov. J. Plasma Phys.* 2 (1976) 257.
- [30] C. Sulem, P.L. Sulem, *The Nonlinear Schrödinger Equation*, Springer-Verlag, New York, 1999.
- [31] V.I. Talanov, Self focusing of wave beams in nonlinear media, *Sov. Phys. JETP Lett.* 2 (1965) 138.
- [32] J.P. Torres, L. Torner, I. Biaggio, M. Segev, Tunable self-action of light in optical rectification, *Opt. Commun.* 213 (2002) 351.
- [33] F. Vidal, T.W. Johnston, Electromagnetic beam breakup: Multiple filaments, single beam equilibria, and radiation, *Phys. Rev. Lett.* 77 (1996) 1282.
- [34] S. Vlasov, V. Petrishchev, V. Talanov, Averaged description of wave beams in linear and nonlinear media, *Radiophys. Quant. Elec.* 14 (1971) 1062 (1070 in English).
- [35] M.I. Weinstein, Nonlinear Schrödinger equations and sharp interpolation estimates, *Commun. Math. Phys.* 87 (1983) 567.
- [36] G.B. Whitham, *Linear and Nonlinear Waves*, Wiley, New York, 1974.